



Published in final edited form as:

Biochemistry. 2006 December 5; 45(48): 14263–14274.

Fatty acid-specific fluorescent probes and their use in resolving mixtures of unbound free fatty acids in equilibrium with albumin†

Andrew H. Huber[‡], J. Patrick Kampf^{‡,§}, Thomas Kwan[‡], Baolong Zhu[‡], and Alan M. Kleinfeld^{‡,§,*}

[‡]*FFA Sciences LLC*

[§]*Torrey Pines Institute for Molecular Studies*

Abstract

We report the first measurements to profile mixtures of unbound free fatty acids. Measurements utilized fluorescent probes with distinctly different response profiles for different free fatty acids (FFA). These probes were constructed by labeling site-specific mutants of the rat intestinal fatty acid binding protein (rI-FABP) with acrylodan. The probes were produced and screened by high throughput methods and from more than 30,000 such probes we selected 6 that together have sufficient specificity and sensitivity to resolve the profile of unbound FFA (FFA_u) in mixtures of different FFA_u . We developed analytical methods to determine the FFA_u profile from the fluorescence (ratio) response of the different probes and used these methods to determine FFA_u profiles for mixtures of arachidonate, linoleate, oleate, palmitate and stearate in equilibrium with bovine serum albumin (BSA). Measurements were performed using mixtures with a range of total FFA_u concentrations, including 0.9 nM, which is similar to normal plasma levels. We also measured single FFA binding isotherms for BSA and found that binding was well described by 6-7 sites with the same binding constants (K_d). The K_d values for the FFA (4 to 38 nM) were inversely related to the aqueous solubility of the FFA. We constructed a model with these parameters to predict the FFA_u profile in equilibrium with BSA and found excellent agreement between the profiles measured using the FFA probes and those calculated with this model. These results should lead to a better understanding of albumin's role in buffering FFA_u and to profiling FFA_u in intra and extracellular biological fluids.

Keywords

unbound free fatty acids; fatty acid binding proteins; fluorescent probes; site-specific mutants; high throughput screening; fatty acid profiling; binding affinities; bovine serum albumin

Metabolomics is advancing rapidly as a result of new technologies and the expanding interest in systems biology (1). This advance is being driven by the recognition that physiologic phenotype is essentially a reflection of the metabolic profile, and therefore, metabolic profiling should provide an accurate representation of the states of health and disease. The activity of a given metabolite is frequently dictated by its solubility as a “free” or unbound molecule in aqueous bodily fluids. For many metabolites the unbound concentration represents a small fraction of the total, with most of the total metabolite bound in carrier complexes. Total metabolite concentrations are typically measured, but it is the unbound metabolite that interacts

[†]This work was supported by grant DK070314 from the NIH Roadmap Initiative in Metabolomics Technology Development.

*Please send correspondence to Alan M. Kleinfeld, Torrey Pines Institute for Molecular Studies, 3550 General Atomics Court, San Diego, CA 92121. TEL: 858-455-3724, FAX: 858-455-3792, email: akleinfeld@tpims.org..

with targets such as protein receptors and cell membranes (for example (2)). A profiling of unbound metabolite concentrations should therefore provide the most accurate measure of physiologic health.

The issue of profiling unbound rather than total metabolites is especially relevant for the long chain free fatty acids (FFA)¹, which play major roles in signaling, macromolecular structure and energy production. Long chain FFA are sparingly soluble, yet act through extra- and intra-cellular aqueous phases to bind to target macromolecules (2-4). In many instances, FFA-mediated signaling events can be abolished by adding fatty-acid-free bovine serum albumin, which reduces the unbound FFA (FFA_u)² concentration without changing the total FFA concentration (8;9). Total serum concentrations of long chain FFA are in the millimolar range while FFA-protein receptor binding affinities are in the nanomolar range as are FFA_u concentrations (4-7). The hydrophobic nature of FFA and low FFA_u concentrations have made it difficult to measure FFA_u in biological fluids, and thus, total FFA is typically measured even though FFA-dependent signaling events are triggered by unbound rather than total FFA concentrations.

More than 40 different species of FFA with widely different biological activities have been identified in human serum (10). Striking examples of their different biological activities include the induction of apoptosis in various cell types by palmitate (16:0) but not oleate (18:1) (11-13) and the inhibition of cytotoxic T lymphocyte signaling by oleate (OA) but not palmitate (PA) (9;14). In addition, alterations in the profile of total plasma FFA have been reported in association with disease states (10;15-(18).

Plasma FFA_u levels are a reflection of the FFA-albumin binding equilibrium. The affinities of albumin for different FFA can differ by more than 2 orders of magnitude (5;19), and therefore, the equilibrium FFA_u profile will differ from the total profile. FFA_u profiles have not been reported previously because none of the available measurement techniques can resolve the nanomolar quantities of individual FFA_u in the FFA_u mixtures present in aqueous biological fluids. However, measurements of individual FFA_u and/or average values for FFA_u mixtures have been carried out previously using the acrylodan labeled fatty acid binding proteins ADIFAB and ADIFAB2 (7;20).

In the present study, we have developed new fluorescently labeled fatty acid binding proteins (probes) with FFA response profiles distinctly different from those of ADIFAB and ADIFAB2. Together, these new probes have sufficient specificity and sensitivity to resolve individual FFA_u in FFA_u mixtures. The new probes were constructed by labeling site-specific mutants of the rat intestinal fatty acid binding protein (rI-FABP) with acrylodan. More than 30,000 such probes were generated and screened for ligand specificity using high throughput methods. We have selected and further characterized a subset of more than 140 probes that have high sensitivity and specificity for individual FFA. In this study, we describe 6 probes that display specificity for the 5 FFA that are among the most abundant in human plasma: PA, OA, linoleate (LA), stearate (SA) and arachidonate (AA).

¹FABP, fatty acid binding protein; rI-FABP, rat intestinal FABP, ADIFAB, acrylodan labeled rIFABP; ADIFAB2, acrylodan labeled L72A mutant of rI-FABP; BSA, bovine serum albumin; FFA, free fatty acid; FFA_u, unbound FFA; AA: arachidonic acid (20:4 Δ5,8,11,14); LNA: linolenic acid (18:3Δ9,12,15); LA: linoleic acid (18:2 Δ9,12); OA: oleic acid (18:1 Δ9); SA: stearic acid (18:0); POA: palmitoleic acid (16:1 Δ9); PA: palmitic acid (16:0).

²FFA are non-esterified or 'free' fatty acids and 'unbound FFA' are aqueous phase monomers of FFA, a state which can be detected by the probes. Because a fatty acid is, by definition, nonesterified the term 'free fatty acid' could be used to denote the unbound fatty acid. Nevertheless, the most common usage refers to non-esterified fatty acids as free fatty acids, primarily to distinguish fatty acids from fatty esters. Because few studies have dealt explicitly with the unbound, aqueous phase monomers, we have in this and in previous studies used FFA_u to emphasize the distinction between the unbound fatty acids in the aqueous phase and those that are protein or lipid bound.

As a first step towards the determination of blood plasma FFA_u profiles, we have used these 6 new probes to profile mixtures of 4 and 5 FFA in equilibrium with bovine serum albumin (BSA). Because there is no independent method to determine FFA_u concentrations, we also calculated the expected profiles from the known amounts of FFA and BSA used to generate the mixtures. These calculations required binding constants for each BSA-FFA interaction and a new BSA-binding model. Our measurements indicate that, to a good approximation, the binding of each of the FFA to BSA can be described in terms of a single class of 6 to 7 independent sites. Using this simple model, we have calculated FFA_u profiles for mixtures of 4 and 5 FFA in equilibrium with BSA and compared these predictions to FFA_u profiles measured with our probes. Good agreement was found between these two independent profiling methods.

Experimental Procedures

Materials

Essentially fatty acid free bovine serum albumin, buffer salts, DNase I, lysozyme, HEPES, His-Select Ni-Affinity Gel, hydroxyalkoxypropyl dextran, N,N-dimethylformamide (DMF) and Triton X-100 were purchased from Sigma-Aldrich (St. Louis, MO). Fatty acid sodium salts were obtained from NuChek Prep (Elysian, MN). ADIFAB and ADIFAB2 were prepared as previously described (21;22) and are available from FFA Sciences LLC (San Diego, CA). Acrylodan was purchased from Invitrogen (Carlsbad, CA). Oligonucleotides were synthesized by Operon Biotechnologies, Inc. (Huntsville, AL). The protein expression vector (pET11d) for mutant rI-FABP was obtained from Novagen (Madison, WI). DNA modification enzymes were from Stratagene (La Jolla, CA) and New England Biolabs (Ipswich, MA). Protein Assay reagents were purchased from Bio-Rad (Hercules, CA).

The following buffers and stocks were used: Measurement Buffer contained 20 mM HEPES, 140 mM NaCl, 5 mM KCl, and 1 mM Na₂HPO₄ at pH 7.4; Storage Buffer was Measurement Buffer plus 0.05% (w/v) sodium azide and 1 mM EDTA; Lysis Buffer contained 50 mM Tris-HCl pH 8, 250 mM NaCl, 5 mM MgSO₄, 5 mM KCl, 1.0 mg/ml lysozyme and 5 µg/ml DNase I; Buffer 1 contained 50 mM Tris, pH 8.0, 200 mM NaCl, and 10 mM imidazole; Elution Buffer contained 15 mM HEPES, pH 7.4, 110 mM NaCl, 4 mM KCl, 1 mM Na₂HPO₄, 100 mM EDTA; BTP Buffer contained 10 mM Bis-Tris Propane, pH 9.3, 100 mM NaCl; Buffer 2 contained 50 mM Tris, pH 8.0, 200 mM NaCl, 15 µM essentially fatty acid free BSA; Buffer 3 contained 10 mM Tris, pH 8.0, 200 mM NaCl; Buffer 4 contained 50 mM Tris-HCl, 5 mM MgCl₂, 200 mM NaCl, pH 8; Buffer 5 contained 75 mM Tris-HCl pH 8.0, 150 mM NaCl, and 250 mM imidazole; and Buffer 6 contained 10 mM BTP, pH 9.3, 50 mM NaCl. All acrylodan stocks were prepared in DMF.

Library Generation

Libraries of mutant rI-FABP proteins were created by *in vitro* site-directed mutagenesis using a PCR overlap extension method (23). All mutant FABP genes encoded a COOH-terminal six-histidine tag. Nco I and BamH I restriction sites were added to 5'- and 3'-ends of the tagged-FABP gene by incorporating them into the 5' and 3'-terminal oligonucleotides for PCR. The Nco I/BamH I-digested library was ligated into Nco I/BamH I-digested pET-11d - vector and *E. coli* strain BL21 (DE3) was transformed with the ligation mixture. Transformed cells were plated onto Luria Broth agar containing 100 µg/ml carbenicillin (LB/carb agar).

Library Pre-screening

Isolated colonies were picked for small-scale growth in 96-position deep-well plates containing 375 µl of LB/carb per well. Cultures were grown overnight and induced the next morning by

adding 125 μ l of a 1.6 mM solution of IPTG in LB/carb. After an additional 4 hours at 37 $^{\circ}$ C, the cells were pelleted by centrifugation and the pellets stored at -80° C.

Cells were lysed by adding 200 μ l of Lysis Buffer to each thawed pellet and subjecting the cells to two freeze-thaw cycles. Cellular debris was pelleted by centrifugation and 150 μ l of lysate supernatant from each well was transferred to a fresh deep-well block. Approximately 30 μ l of a 25% suspension of His-Select Ni-Affinity Gel was added to each well, incubated 10 minutes at room temperature, and the lysate aspirated away. Each bed of Ni-affinity beads was washed once with a 1.4 ml aliquot of Buffer 1. Affinity purified protein was eluted by adding 50 μ l of Elution Buffer to each well and incubating at room temperature for 10 minutes. Eluted protein concentrations were estimated using the BioRad Protein Assay (24). Clones with suitable levels of protein expression were chosen for additional characterization.

Small-scale Purification and Labeling of Mutant FABP

Clones yielding sufficient protein during prescreening were grown overnight in 48-position deep well plates, with each well containing 1.5 ml of LB/carb. Cultures were induced the next morning by adding 1.5 ml of an 800 μ M solution of IPTG in LB/carb. After an additional 4 hours at 37 $^{\circ}$ C, the cells were pelleted by centrifugation and the pellets stored at -80° C.

Cells were lysed by adding 200 μ l of Lysis Buffer to each thawed pellet and putting the samples through two freeze-thaw cycles. Cellular debris was pelleted by centrifugation and 200 μ l of lysate supernatant from each well was transferred to a fresh deep-well block. The lysate from pairs of 48-position blocks were moved to single 96-position deep well blocks for labeling.

Approximately 100 μ l of a 25% slurry of His-Select Ni-Affinity Gel was added to each well, incubated 10 minutes at room temperature, and the lysate discarded. The bed of Ni-affinity beads in each well was washed once with 1.4 ml of Buffer 1 and three times with 1.4 ml aliquots of BTP Buffer. The addition of 500 μ l of 37 $^{\circ}$ C BTP Buffer followed by 5 μ l of 20 mM acrylodan to each well started the labeling reaction. Samples were incubated for 1 hour at 37 $^{\circ}$ C with end-over-end mixing. The beads in each well were washed once with 1.4 ml of Buffer 2 and three times with 1.4 ml aliquots of Buffer 3. Mutant FABP probes were eluted at room temperature with 250 μ l aliquots of Elution Buffer. Probe concentrations were estimated using the BioRad Protein Assay.

Large-scale Purification and Labeling of Mutant FABP

Cultures in LB/carb were grown in baffled shake flasks at 37 $^{\circ}$ C and induced during late log phase by adding IPTG to a final concentration of 200 μ M. Cells were harvested by centrifugation 3 hours after induction and stored at -80° C. Cell pellets were resuspended in 7 ml of Buffer 4 per g of cells and protease inhibitors (2.6 mg phenylmethylsulfonyl fluoride and 28 μ g aprotinin per g of cell pellet) were added to the suspension. DNase I and Triton X-100 were added to final concentrations of 8.75 μ g/ml and 1%(v/v), respectively. Cellular debris was pelleted and the lysate supernatant passed over a His-Select HF Nickel Affinity column. Purified FABP was eluted with Buffer 5. Additional size exclusion and anion exchange chromatography steps provided pure mutant FABP.

Fluorescent probes were generated by slowly adding 20 mM acrylodan to a 100 μ M FABP stock in Buffer 6 until an acrylodan:protein molar ratio of 2:1 was reached. The reaction was incubated at 37 $^{\circ}$ C with constant mixing for the duration of the acrylodan addition and for an hour afterwards. Placing the reaction vessel on ice and neutralizing the reaction pH with HCl terminated the reaction. Unreacted acrylodan was removed with a hydroxyalkoxypropyl dextran column, and the probe was further purified by size-exclusion chromatography, using an XK 26/100 Superdex 200 Prep-grade column (GE Healthcare components) equilibrated

with Measurement Buffer. The labeling efficiency of monomer peak fractions was checked by reversed phase column chromatography (Grace-Vydac, 214MS54-C4) and by measuring fluorescent R -values (see Equation 1). Suitable fractions were pooled to create a final probe stock. EDTA and sodium azide were added as preservatives at final concentrations of 1 mM and 0.05% (w/v), respectively.

Phenotypic Screening

Probe FFA_u response profiles (phenotypes) were determined in a 384-well format by measuring the fluorescence response of each probe to 7 different FFA. Screening success was critically dependent upon the preparation of FFA solutions with precisely defined and highly reproducible unbound concentrations ([FFA_u]). To avoid pitfalls resulting from the low solubility of long chain fatty acids and their propensity for non-specific binding to surfaces, BSA was used as a buffering agent. Reliable [FFA_u] values were generated by using FFA–BSA complexes as described previously (3). FFA–BSA complexes were prepared by slow addition of alkaline (pH > 11) stocks of 50 mM fatty acid sodium salts to stirred solutions of 600 μM BSA in Measurement Buffer at 37°C. FFA sodium salts were used because they dissolve more rapidly than the neat acid. The alkaline stocks of PA and SA were warmed to 70°C before addition to the BSA solution as described in (25). Desired stock FFA_u concentrations, which ranged from 10 to 1500 nM depending on FFA type, were achieved through an iterative process of fatty acid addition and measurement of [FFA_u] with ADIFAB2. The complexes were diluted to 12 and 6 μM BSA in Measurement Buffer for screening and measurement with ADIFAB2, respectively.

The fluorescence ratio (R) of each well in the 384-well plate was measured at emission wavelengths 457 and 550 nm upon excitation at 375 nm. R is defined by [Equation 1] where I_{λ}^{Probe} is the intensity of the well at emission wavelength λ nm with probe present and I_{λ}^{Blank} is the intensity without probe present (21). Emission wavelengths 457 and 550 nm were chosen to minimize the effects of absorption by hemoglobin on R , which is necessary for profiling FFA_u in blood, a future use for these probes (7;26). The absorbance of hemoglobin is equivalent at each of the two wavelengths and will cancel in R . Each screening well contained 0.5 to 10 μM probe and either fatty acid free BSA or FFA–BSA in 0.1 mL Measurement Buffer. The magnitude of the ratio measurement error depended upon probe intensity and was typically ≤ 2%.

$$R = \frac{I_{550}^{Probe} - I_{550}^{Blank}}{I_{457}^{Probe} - I_{457}^{Blank}} \quad (1)$$

With each probe, the difference (ΔR) between the ratio with and without each fatty acid was determined and compared to that for the reference probe ADIFAB2 (ΔR_{AD2}) by dividing the ratio changes ($\rho_i \equiv \Delta R / \Delta R_{AD2}$). The set of ρ_i for all FFA screened defined the phenotype for a given probe. Probes for which all ρ_i values were close to 1 had responses similar to ADIFAB2 and were generally not characterized further. Likewise, probes for which all ρ_i values were close to 0 were not useful FFA probes because they were not responsive to the screened FFA. Probes that showed significantly nonuniform ρ_i profiles were prepared at larger scale and a detailed characterization of their FFA binding and spectral properties was performed.

Probe Calibration

A complete calibration of each probe chosen for large scale preparation was performed, at 22°C, to determine the dissociation and fluorometric constants of Equation 2 which relates [FFA_u] to R .

$$[FFA_u] = K_d \cdot Q \cdot \frac{(R - R_0)}{(R_m - R)} \quad (2)$$

In Equation 2, R_0 is the value of R when no FFA is present, Q is the ratio of the intensity at 457 nm when no FFA is present to that when the probe is saturated with FFA, K_d is the dissociation constant, and R_m is R at saturation. Probe calibration was a two-step process involving the titration of probes with (i) un-buffered and (ii) BSA-buffered FFA stocks with known total ($[FA_t] = [FFA_{bound}] + [FFA_u]$) and unbound FFA concentrations, respectively. The un-buffered titrations were performed as previously described (21;27). Briefly, R was measured as a 1 μ M probe solution was titrated to saturation with small aliquots of a 100 to 250 μ M FFA stock. The emission spectra of each probe were also recorded during titration with FFA to assess the spectroscopic change corresponding to the bound and free forms of the probe.

For a fully labeled probe, such as ADIFAB, a nonlinear fit to the titration data reveals the full set of fluorometric constants. Mutant probe preparations often had significant amounts of unlabeled protein. In these cases the effective FFA concentration for the titration was unknown because the affinity of the unlabeled protein was unknown, and therefore an accurate determination of K_d was not possible. However, an accurate $[FFA]$ value was not needed to determine Q and R_m and these values were determined from the first calibration step.

In the second step, the buffering properties of BSA were exploited to complete the calibration. A series of FFA–BSA complexes with increasing $[FFA_u]$ (1 nM to 4 μ M as determined by ADIFAB2), were prepared for each FFA as described above. The complexes were then diluted 100 fold in Measuring Buffer containing 0.5 μ M probe, and R was measured for each complex. Because BSA buffers $[FFA_u]$, the presence of unlabeled protein did not alter $[FFA_u]$ as long as the albumin concentration was significantly greater than the protein concentration. Therefore, the resulting R versus $[FFA_u]$ data was used to accurately determine K_d for a fixed Q . At least two calibrations with each of the 7 FFA were performed for each probe. The accuracy of the calibrations was checked with defined FFA–BSA complexes prior to the mixture measurements, and small corrections were made when necessary.

FFA–BSA Binding Isotherms

The binding affinities of individual FFA for BSA were determined using ADIFAB2 as previously described for ADIFAB (5). ADIFAB2 has approximately 10 fold higher affinities than ADIFAB and therefore provides more accurate $[FFA_u]$ values at low concentrations. Small aliquots of a 0.25 to 1 mM FFA solution were added to continuously stirred Measurement Buffer containing 1 to 6 μ M albumin and 0.25 to 0.5 μ M ADIFAB2 at 22°C. The fluorescence ratio was measured following each addition, from which $[FFA_u]$ was determined using (Equation 2). The amount of FFA bound to albumin was calculated by subtracting the unbound FFA and the FFA bound to ADIFAB2 (5) from the total FFA added.

Resolving Mixtures of Fatty Acids

Albumin-FFA mixtures with a defined total $[FFA_u]$ ($= \sum_{i=1}^n [FFA_{ui}]$) were obtained by mixing together different volumes of single FFA–BSA complexes, each with $[FFA_u]$ equal to the desired total $[FFA_u]$. For example, to make a 1:1:1 tertiary mixture of LA, OA and PA at a total $[FFA_u]$ concentration of 4 nM, we mixed together equal portions of individual LA–BSA, OA–BSA and PA–BSA complexes, each with an $[FFA_u]$ concentration of 4 nM. Although equal volumes of the complexes were mixed, the $[FFA_u]$ distribution was not uniform because each FFA has a different binding affinity for albumin.

FFA_u measurements for the FFA-BSA mixtures were taken with a suite of probes having different FFA specificities. Profiling requires measurement with at least one probe per FFA specie. The response, R , of a probe to a sample with multiple FFA is described by Equation 3, where R_0 , R_{mi} , Q_i and K_{di} are probe spectral and binding constants as described in the previous section and the subscript i denotes the different FFA.

$$\sum_{i=1}^n \frac{[FFA_{ui}]}{Q_i \cdot K_{di}} (R_{mi} - R) = R - R_0 \quad (3)$$

Equation 3 is an extension of Equation 2, which describes the response of a single probe to a single fatty acid. Profiling mixtures with multiple probes requires a set of equations, linear in FFA_{ui} , that describe the response of each probe to the mixture of FFA. This set of equations can be expressed in matrix form [(Equation 4)] where subscripts a , b , c , etc. refer to different probes and subscripts 1 , 2 , 3 , etc. refer to different FFA. The matrix can be expanded to include any number of FFA (n) or probes (z) where $z \geq n$. The FFA_{ui} distribution within a mixture was determined by measuring the response, R , of each probe and solving Equation 4. We estimated the errors in the FFA_{ui} values assuming a 1% error in the R values and calculated the resulting FFA_{ui} using Equation 4. This estimation yields uncertainties in FFA_{ui} that ranged between 1 and 30% (see Table 6) and is thought to be conservative because the uncertainties in R are less than 1 %.

$$\begin{bmatrix} \frac{R_{m1a}-R_a}{Q_{1a}K_{d1a}} & \frac{R_{m2a}-R_a}{Q_{2a}K_{d2a}} & \frac{R_{m3a}-R_a}{Q_{3a}K_{d3a}} & \dots & \frac{R_{mna}-R_a}{Q_{na}K_{dna}} \\ \frac{R_{m1b}-R_b}{Q_{1b}K_{d1b}} & \frac{R_{m2b}-R_b}{Q_{2b}K_{d2b}} & \frac{R_{m3b}-R_b}{Q_{3b}K_{d3b}} & \dots & \frac{R_{mnb}-R_b}{Q_{nb}K_{dnb}} \\ \frac{R_{m1c}-R_c}{Q_{1c}K_{d1c}} & \frac{R_{m2c}-R_c}{Q_{2c}K_{d2c}} & \frac{R_{m3c}-R_c}{Q_{3c}K_{d3c}} & \dots & \frac{R_{mnc}-R_c}{Q_{nc}K_{dnc}} \\ \vdots & \vdots & \vdots & \ddots & \vdots \\ \frac{R_{m1z}-R_z}{Q_{1z}K_{d1z}} & \frac{R_{m2z}-R_z}{Q_{2z}K_{d2z}} & \frac{R_{m3z}-R_z}{Q_{3z}K_{d3z}} & \dots & \frac{R_{mnz}-R_z}{Q_{nz}K_{dnz}} \end{bmatrix} \begin{bmatrix} [FFA_{u1}] \\ [FFA_{u2}] \\ [FFA_{u3}] \\ \vdots \\ [FFA_{un}] \end{bmatrix} = \begin{bmatrix} R_a - R_{0a} \\ R_b - R_{0b} \\ R_c - R_{0c} \\ \vdots \\ R_z - R_{0z} \end{bmatrix} \quad (4)$$

Fluorescence Instrumentation

Probe calibrations, preparation of FFA-BSA complexes, and FFA-BSA binding isotherms were performed on either an SLM 8100 or a Spex Fluorolog-3 spectrofluorometer. Phenotypic screening was completed on a Spex MicroMax 384 fluorescence plate reader. A custom insulated chamber with circulating cold water was used to maintain a temperature of $22 \pm 1^\circ$ C within the plate reader.

Measurements used to resolve mixtures of FFA were performed with a hand-held ratio fluorometer, the “FFA_u Meter” (FFA Sciences LLC), designed specifically for use with ADIFAB2 and analogous probes. This instrument uses an epifluorescence configuration and cylindrical glass cuvettes containing sample volumes of 200 μ L. A light-emitting diode provides excitation at 375 nm and two photodiodes detect emission through bandpass filters, centered at 457 and 550 nm. FFA_u Meter measurements used 200 μ l of Measurement Buffer, 1.5 μ M of the probe and 1% by vol. of the FFA-BSA mixture. The ratio (R) was measured three times and the average values were used with Equation 4 to determine the FFA_{ui} distribution. The average standard deviation in the ADIFAB2 ratio using this instrument was 0.3%.

Result

FFA Specificities of Mutant Probes

Screening approximately 30,000 mutant probes with 7 different FFA yielded a large number of probes with novel phenotypes, and we chose approximately 140 of these probes for detailed

characterization. The FFA_u response profiles (p_i values) were used to select a subset of 6 probes with significantly different and complementary responses to individual FFA. This subset revealed improved specificity for OA, PA, SA, LA, and AA relative to the ADIFAB2 template. These probes, which have 3 to 6 substitutions in the cavity/portal regions of rat I-FABP, were used to resolve mixtures of 4 and 5 FFA in complex with BSA (Table 1).

The 6 probes have different fluorescence responses to FFA binding as indicated by their different emission spectra Figure 1. With the exception of L1P8H2, FFA binding to all of the probes revealed an emission red shift of 20 to 80 nm that resulted from an intensity decrease between 425 and 480 nm and either an increase or no change in intensity between 500 and 550 nm. The L1P8H2 probe exhibits a negative response (R value decreases upon FFA binding) characterized by a blue shift of 50 nm that reflects an intensity increase at about 450 and a decrease at about 515 nm. For all probes, the ratio (R) of the intensity at 550 nm to that at 457 nm provides a direct measure of the fraction of bound probe. Therefore, Equation 2 can be used to determine the unbound FFA concentration from the measurement of R with a calibrated probe (Methods). Probes were calibrated for each FFA (Table 2) by determining their binding affinities (K_d) and fluorescent parameters (R_o , Q and R_m), as described in Methods. The specificity and magnitude of the response of a particular probe to a given FFA, reflects both binding and fluorescent parameters. For example, L10P7A4 has virtually identical K_d values for OA and LA but the response to LA is greater because its Q and R_m values are substantially larger than those for OA.

Specificity is best gauged by rearranging Equation 2 and comparing the calculated fractional change in R ($\Delta R/R_o$) between probes for each FFA_u. This was done using the calibration parameters of (Table 2) for 1 nM FFA_u and the results for the 6 mutant probes and ADIFAB2 reveal the range of specificities generated by the mutation/screening procedures (Figure 2). The results for each probe are displayed in order of FFA solubility, from the most (POA) to the least (SA) soluble FFA. As discussed previously (21;22), the ADIFAB2 response directly reflects the FFA solubility, revealing a monotonic increase in response from POA (1%/nM) to SA (20%/nM). In contrast, both L1P8H2 and L13P7B4 respond most to OA; L2P22G6 is most sensitive to PA; L10P7A4 responds almost equally well to AA and LA; and L18P5G12 shows LA specificity. Like ADIFAB2, L11P7B3 is most sensitive to SA but with a more than 4 fold larger response.

Fatty acid - BSA binding isotherms

BSA binding affinities, which are required for the BSA binding model, were measured for the five fatty acids, AA, LA, OA, PA, SA as well as POA and LNA. The dissociation constant ($K_{d_i}^a$) and the number of binding sites (M) for each FFA (Table 3) were determined using Equation A5 as described in the Appendix. Binding isotherms represented as the concentration of fatty acid bound divided by the total albumin concentration as a function of [FFA_u] are shown in (Figure 3). In all cases the binding isotherms reveal a sharp rise in the concentration of fatty acid bound at low FFA_u and asymptotic saturation at high FFA_u.

The results of this analysis indicate that a single-class model (Appendix) with 6 to 7 binding sites provides an excellent description of FFA binding to BSA (Figure 3). A two-class analysis does not improve the fit to the data and yields virtually identical affinities for both classes that are in turn equivalent to the affinities of the single class model. Binding affinities increase with decreasing aqueous solubility of the FFA (Table 3). Small deviations from single class fits appear at the highest FFA_u levels, possibly resulting from binding to additional low affinity sites on albumin, nonspecific binding of FFA to the cuvette, or a combination of these events.

Binding of Mixtures of Different Fatty Acids with BSA

We used our new probes (Table 1 and Figure 2) to resolve the FFA_u distributions of mixtures of fatty acids in equilibrium with BSA. Measurements were performed using mixtures of four and five FFA interacting with BSA (Tables 4, 5 & 7). The measured distributions were compared with the predictions of the single-class BSA-binding model, which are indicated as “Model” in Tables 4, 5 & 7.

Two separate mixtures (1:1:1:1 and 30:35:20:15) of the four FFA, AA, OA, PA, and SA, were used at total FFA_u concentrations of 3 and 20 nM. The FFA_u distributions resulting from the interaction of BSA with these two mixtures were resolved with the four probes L1P8H2, L2P22G6, L10P7A4 and L11P7B3. Excellent agreement was observed between measured and the model predicted FFA_u distributions, which are presented as the concentration and the mol % (X) of each FFA_u (Table 4). The average magnitude of the percentage difference between measured and model-predicted FFA_{ui} values was 10 % (the average was -3%) with the largest difference (25%) occurring at the lowest concentration component (SA at 0.31 nM).

Mixtures (1:1:1:1:1 and 20:25:30:15:10) of the five fatty acids AA, LA, OA, PA and SA at total FFA_u concentrations of 3 and 20 nM were resolved using the probes L1P8H2, L2P22G6, L10P7A4, L11P7B3 and L18P5G12 (Table 5). Additional mixtures (1:1:1:1:1, 20:25:30:15:10 and 25:20:33:19:3) with 0.9 nM total FFA_u were resolved using the L13P7B4 probe instead of L1P8H2 because L13P7B4 has better OA specificity than L1P8H2. The 25:20:33:19:3 mixture was chosen to approximate plasma FFA_u levels (20). These mixtures, comprising 5 FFA species, yielded profiles with the expected trends for the different FFA mixtures. The experimental uncertainties in the determination of the FFA_{ui} values for these mixtures were determined (Table 6) as described in Methods and are representative of all the mixtures investigated in this study.

The results also reveal excellent agreement between experiment and model distributions with average absolute values of the percentage differences ranging from 10% for the 3 and 20 nM mixtures to 13% for the 0.9 nM mixtures. The largest differences in FFA_{ui} between the experiment and model are for OA and PA in the 0.9 nM mixtures and partly reflect the estimated experimental uncertainties of Table 6 and the small dynamic range of the L13P7B4 probe (Table 2).

Differences in the FFA_u distributions for the different mixtures roughly follow the trend expected from the differences in binding affinities for BSA (Table 3). For the equal mixtures, [FFA_u] is largest for AA and smallest for SA, even though [FA_i] for SA is largest and that for AA is smallest (Table 7). As mentioned above, the [FFA_u] values for the single FFA-BSA complexes were the same before mixing. However, because SA has the highest affinity for BSA of the five FFA considered here, more SA needs to be added to the BSA for the stock to achieve the desired [FFA_u] value. The same [FFA_u] value is achieved with much less AA because it has the lowest affinity for BSA of the five FFA. For similar reasons, the relative fraction of AA tends to increase and that of SA decreases with increasing total [FFA_u]. For the most part, the differences in [FFA_u] distributions between the equal and 30:35:20:15 mixtures reflect the larger amounts of unsaturated (AA, OA) relative to saturated (PA, SA) FFA_u in the mixtures.

Discussion

We have developed high throughput methods to generate large numbers of fluorescent probes derived from rI-FABP and to determine the FFA response profiles of the probes. A subset of probes with high specificity and sensitivity for different FFA was used to measure the distribution of FFA_u in BSA-buffered mixtures of some of the physiologically most abundant

FFA. In addition, we determined the binding isotherms for single FFA interacting with BSA and used these results to formulate a single class BSA-binding model that accurately predicted the measured FFA_u distribution of equilibrated FFA-BSA mixtures. This is the first report of measurements that resolve unbound FFA concentrations in mixtures of different FFA, and our results suggest that it should be possible to measure the $[\text{FFA}_u]$ profile in biologically relevant fluids.

Probe generation and screening

In previous studies, we measured the $[\text{FFA}_u]$ of single FFA or the average $[\text{FFA}_u]$ in mixtures of different FFA using two different fluorescent probes: ADIFAB (21) and ADIFAB2 (7;22; 26). ADIFAB is fluorescently labeled wild-type rI-FABP and ADIFAB2 is a fluorescently labeled L72A mutant. The L72A mutant was chosen out of several tested (28;29) because the FFA binding affinities for the unlabeled protein were about 10 fold larger than for the wild-type protein. This difference was retained after fluorescent labeling, with ADIFAB2 binding affinities approximately 10 fold greater than those of ADIFAB. Moreover, the relative binding affinities and the relative fluorescence responses to different FFA were virtually identical for ADIFAB and ADIFAB2.

Unlike ADIFAB and ADIFAB2 (28;29), the fluorescence responses of most rI-FABP mutants are not simply correlated with the FFA binding affinities of the unlabeled proteins. For example, we did not predict from protein affinities that probes would reveal a negative response (L1P8H2) and that the fluorescence response of a given probe would be FFA specific because the fluorescence parameters Q and R_{max} would be different for different FFA (Table 2). These results indicate that in searching for probes whose responses are specific for certain ligands, the search must be conducted using the probes rather than the unlabeled protein.

Single class binding to BSA

Although the low solubility of long chain FFA and the rapid kinetics of their interactions with BSA place severe limitations on the types of methods that can be used, binding parameters for FFA interacting with BSA have been determined using several techniques (5;19;30-35). There is reasonable agreement among all studies that have reported BSA binding affinities after 1990 and these affinities are higher than those published in earlier studies (30). For example, in the studies of Bojesen and Bojesen (31;33;34), who measured PA, OA, LA and AA binding to BSA at 23°C with FFA/BSA ratios up to 1.5, the results are consistent with a single class of 3 to 4 independent sites. Bojesen and Bojesen obtained K_d values at 23°C for PA, OA, LA and AA of 15, 3, 10 and 16 nM, which are reasonably similar to the respective values of 8, 6, 13 and 16 nM, obtained in the present study (Table 3). In addition, Rose et al (32) and Elmadhoun et al (35) both find good agreement with the stepwise BSA binding affinities published in our earlier study using ADIFAB (5).

In our previous study (5) we used ADIFAB to determine binding isotherms for long chain FFA interacting with BSA and analyzed the binding isotherms using the accepted step-wise model. We noted, however, that it was unclear whether the distinct binding constants for each of the 6 sites represented the actual binding constants (5). We have reanalyzed these earlier results and find that the single class model yields as good a fit as the step-wise analysis (data not shown). These results are further supported by a more recent ADIFAB study in which we observed that OA binding to BSA at 37°C was well described by a single class of about 5 sites with a K_d of 14 nM (36). Moreover, we also measured dissociation rate constants for FFA-BSA complexes and found they were independent of the $[\text{FFA}]/[\text{BSA}]$ ratio and that dissociation was consistent with a single rate constant (36). Rate constants were determined for PA, SA, OA, LA, LNA and AA, and, with the exception of LNA, the changes in k_{off} with FFA type are well correlated with the changes in K_{di}^a with a *i*th FFA type (Table 3). These

equilibrium and kinetic results have shown that rate constants and equilibrium binding constants for FFA-BSA interactions are both consistent with single classes of multiple sites.

The accuracy of the FFA-BSA binding isotherms, and therefore the single class model, depends directly on the accuracy with which FFA_{u} concentrations can be determined. The fluorescence probe method is quite simple, involving only the addition of probe to the FFA-BSA sample, a fluorescence measurement, and the calculation of the FFA_{u} concentration from the ratio of fluorescence intensities. We are not aware of any factors, other than those described in the methods, that compromise the accuracy of our FFA_{u} measurements with ADIFAB2 or any other fluorescent probe in BSA buffered stocks. Because all new probes were calibrated with ADIFAB2 to yield the same FFA_{u} concentration for each FFA-BSA complex, all probe-based [FFA_{u}] measurements are at least as reliable as those with ADIFAB2. We therefore expect the FFA_{ui} profile to be accurate no matter what binding model applies to BSA. Moreover, the remarkable agreement between the predicted and measured profiles strongly suggests that both measurement and model are correct. The model values for FFA_{ui} are predictions of Equation (A6) which are based upon the independently determined K_{di} values of Table 3.

A single class binding model would seem to be inconsistent with published crystallographic structures of FFA-human serum albumin complexes in which 7 chemically distinct binding sites are observed for long chain FFA (37). However, these structures reveal little about the binding affinities of these chemically distinct sites. NMR studies of ^{13}C labeled FFA have revealed at least 2-3 distinct binding environments for BSA, even at the lowest [FFA]/[albumin] ratios (38;39). However, it should be noted that NMR can detect binding interactions with FFA exchange rates up to approximately 30 ms (40), extremely fine temporal resolution compared to that obtained with kinetic and binding measurements carried out on a 1-600 s time scale. We propose that our dissociation and binding measurements reflect an averaging of the microscopic parameters for FFA-BSA interactions. Thus, while our single class model accurately predicts our experimentally determined FFA_{u} values, these results do not preclude the existence of multiple microscopic binding affinities.

The observed inverse relationship between BSA binding affinity and FFA solubility is consistent with our previous studies of FFA binding to wild type FABPs (41). In those studies, we showed that the total free energy change for the transfer of FFA from water to a relatively non-polar FABP binding cavity reflected the sum of three free energy components: increased water entropy due to removal of hydrophobic FFA, decreased FFA entropy due to its immobilization in the binding pocket, and increased enthalpy from FFA-amino acid interactions. We concluded that during FABP-FFA complex formation, the FFA and water entropy changes tend to offset each other, resulting in a modest overall entropic change that essentially reflects FFA solubility. Thus, the overall free energy of binding is predominantly enthalpic, with a smaller but significant entropic component. The inverse relationship between FFA solubility and BSA binding affinity presented here may also reflect the contribution of a net positive entropy change in which the increase in water entropy is partially compensated by the FFA entropy loss upon binding to BSA.

FFA_{u} profiling

To our knowledge, no other method has been reported for determining the FFA_{u} distribution in a mixture of FFA. Although methods exist to measure the distribution of total (albumin bound and unbound) FFA, this profile differs considerably from the FFA_{ui} profile because of differences in FFA-BSA binding affinities. This difference is illustrated in Table 7 where the measured and model-predicted FFA_{u} distributions are shown with the predicted and experimentally determined total FFA distributions for two of the mixtures of Table 5. These results reveal, for example, that similar FFA_{u} values for SA and AA can only be achieved when

the total SA concentration is substantially higher than the total AA concentration, as expected from the difference in SA and AA binding affinities.

In addition to its greater physiologic relevance, the determination of the FFA_u profile has a number of important advantages over the total distribution methods, especially for biologic fluids such as blood plasma. FFA_u profiling using the fluorescent probes, for example in blood plasma, requires little sample preparation. In contrast, measuring the total FFA distribution requires extensive procedures to extract and separate the lipid components using organic solvents that can themselves alter the FFA distribution. Probe-based measurements require less sample because the measurements are performed directly in 100-fold diluted plasma (20;27) and the measurements are amenable to high throughput techniques such as fluorescent scanning in multi-well plates. On the other hand, probe specificity must be carefully investigated to account for potential interferents in biologic fluids. These and other issues are being investigated in our ongoing efforts to use these and other probes to help distinguish different disease states in human blood specimens

APPENDIXA Model for BSA-Fatty Acid Interactions

Our probe-based method is currently the only means for determining the FFA_u distribution of a mixture comprising multiple FFA in equilibrium with BSA. We have therefore developed a simplified FFA–BSA binding model to help verify our experimentally determined FFA_u distributions. We have assumed that the binding reactions of n different types of FFA with albumin molecules containing M binding sites is reversible and can be represented by the following set of reactions:



where A_f is the concentration of free albumin sites, FFA_{ui} is the concentration of unbound FFA of type i and A_{bi} is the concentration of albumin sites bound with species i . We made the additional assumptions that for each type of FFA all M binding sites are independent and have equal affinities.

According to this model, the albumin dissociation constant (K_{di}^a) for FFA of type i binding to each of the M sites is,

$$K_{di}^a = \frac{[A_f] \cdot [FFA_{ui}]}{[A_{bi}]} \quad (\text{A2})$$

The total albumin (protein) concentration A_t can be expressed in terms of the concentrations of free and bound sites as,

$$[A_t] = \frac{1}{M} \left([A_f] + \sum_{i=1}^n [A_{bi}] \right) \quad (\text{A3})$$

Equations A2 and A3 together with $[A_{bi}] = [FA_{ti}] - [FFA_{ui}]$, where FA_{ti} is the total FFA of type i , yield Equation (A4) which can be used to solve for A_f in terms of the known quantities FA_{ti} , A_t and (K_{di}^a),

$$[A_t] = \frac{[A_f]}{M} \left(1 + \sum_{i=1}^n \frac{[FA_{ti}]}{K_{di}^a + [A_f]} \right) \quad (\text{A4})$$

where FA_{ti} and A_t were determined from the concentration of the fatty acid and albumin stocks, respectively.

The (K_{di}^a) values were obtained from measurements of single FFA binding isotherms by expressing the albumin bound FFA (A_b) as a function of FFA_u according to

$$\frac{[A_b]}{[A_t]} = \frac{M \cdot [FFA_u]}{K_{di}^a + [FFA_u]} \quad (\text{A5})$$

A nonlinear fit to Equation A5 was used to determine (K_{di}^a). We chose not to use a Scatchard analysis because the most relevant region of the binding isotherm for this study is at small FFA/albumin ratios and the Scatchard transformation generates large uncertainties in this region (42). MLAB, a mathematical and statistical modeling program, was used to solve Equation A4 numerically for A_f , and the FFA_{ui} distribution was then calculated from Equation A6 as,

$$[FFA_{ui}] = \frac{K_{di}^a \cdot [FA_{ti}]}{[A_f] + K_{di}^a} \quad (\text{A6})$$

A simple analytical solution for the FFA_{ui} distribution can be obtained that provides an approximation valid under typical physiologic conditions. Because the albumin concentrations are on the order of micromolar and binding affinities are in the nanomolar range, $A_f \gg K_{di}^a$ and Equations A4 and A6 can be reduced to Equations A7 and A8, respectively. The resulting equations can be combined to give the approximate FFA_{ui} profile (A9).

$$[A_t] \approx \frac{1}{M} ([A_f] + [FA_{ti}]) \quad (\text{A7})$$

$$[FFA_{ui}] \approx \frac{K_{di}^a \cdot [FA_{ti}]}{[A_f]} \quad (\text{A8})$$

$$[FFA_{ui}] \approx \frac{K_{di}^a \cdot [FA_{ti}]}{M \cdot [A_t] - [FA_{ti}]} \quad (\text{A9})$$

Equation (A9) predicts an FFA_{ui} distribution that is within 0.01% of the values computed using Equations (A4 & A6) under most physiologic conditions where the high affinity FFA binding sites on albumin are rarely saturated. If only the relative amount of each FFA ($\beta_i = [FA_{ti}]/[FA_t]$) is known, the relative amount of each unbound FFA ($\alpha_i = [FFA_{ui}]/[FFA_u]$) can be determined from the albumin dissociation constants for each FFA (A10).

$$\alpha_i = \frac{\beta_i \cdot K_{di}^a}{\sum_{i=1}^n \beta_i \cdot K_{di}^a} \quad (\text{A10})$$

References

1. Goodacre R. Metabolomics - the way forward. *Metabolomics* 2005;1:1–2.
2. Sorrentino D, Robinson RB, Kiang CL, Berk PD. At physiologic albumin/oleate concentrations oleate uptake by isolated hepatocytes, cardiac myocytes, and adipocytes is a saturable function of the unbound oleate concentration. *J. Clin. Invest* 1989;84:1325–1333. [PubMed: 2794064]

3. Cupp D, Kampf JP, Kleinfeld AM. Fatty acid:albumin complexes and the determination of long chain free fatty acid transport across membranes. *Biochemistry* 2004;43:4473–4481. [PubMed: 15078093]
4. Kampf JP, Kleinfeld AM. Fatty acid transport in adipocytes monitored by imaging intracellular FFA levels. *J. Biol. Chem* 2004;279:35775–35780. [PubMed: 15199061]
5. Richieri GV, Anel A, Kleinfeld AM. Interactions of long chain fatty acids and albumin: Determination of free fatty acid levels using the fluorescent probe ADIFAB. *Biochemistry* 1993;32:7574–7580. [PubMed: 8338853]
6. Richieri GV, Ogata RT, Kleinfeld AM. Equilibrium constants for the binding of fatty acids with fatty acid binding proteins from intestine, heart, adipose, and liver; measured with the fluorescence probe ADIFAB. *J. Biol. Chem* 1994;269:23918–23930. [PubMed: 7929039]
7. Apple FS, Kleinfeld AM, Adams JE. Unbound Free Fatty Acid Concentrations Are Increased in Cardiac Ischemia. *Clinical Proteomics* 2004;1:41–44.
8. Poitout V. The ins and outs of fatty acids on the pancreatic beta cell. *Trends Endocrinol. Metab* 2003;14:201–203. [PubMed: 12826323]
9. Kleinfeld AM, Okada C. Free fatty acid release from human breast cancer tissue inhibits cytotoxic T lymphocyte-mediated killing. *J. Lipid Res* 2005;46:1983–1990. [PubMed: 15961785]
10. Yli-Jama P, Meyer HE, Ringstad J, Pedersen JI. Serum free fatty acid pattern and risk of myocardial infarction: a case-control study. *J Intern. Med* 2002;251:19–28. [PubMed: 11851861]
11. de Vries JE, Vork MM, Roemen TH, De Jong YF, Cleutjens JP, van der Vusse GJ, van Bilsen M. Saturated but not mono-unsaturated fatty acids induce apoptotic cell death in neonatal rat ventricular myocytes. *J. Lipid Res* 1997;38:1384–1394. [PubMed: 9254064]
12. Listenberger LL, Ory DS, Schaffer JE. Palmitate-induced apoptosis can occur through a ceramide-independent pathway. *J. Biol. Chem* 2001;276:14890–14895. [PubMed: 11278654]
13. Hickson-Bick DL, Sparagna GC, Buja LM, McMillin JB. Palmitate-induced apoptosis in neonatal cardiomyocytes is not dependent on the generation of ROS. *Am. J Physiol Heart Circ. Physiol* 2002;282:H656–H664. [PubMed: 11788415]
14. Richieri GV, Kleinfeld AM. Free fatty acid perturbation of transmembrane signaling in cytotoxic T lymphocytes. *J. Immunol* 1989;143:2302–2310. [PubMed: 2789260]
15. Lorentzen B, Drevon CA, Endresen MJ, Henriksen T. Fatty acid pattern of esterified and free fatty acids in sera of women with normal and pre-eclamptic pregnancy. *Brit. J. Obstetrics and Gynecology* 1995;102:530–537.
16. Rodriguez de Turco EB, Belayev L, Liu Y, Busto R, Parkins N, Bazan NG, Ginsberg MD. Systemic fatty acid responses to transient focal cerebral ischemia: influence of neuroprotectant therapy with human albumin. *J Neurochem* 2002;83:515–524. [PubMed: 12390513]
17. Yli-Jama P, Seljeflot I, Meyer HE, Hjerkin EM, Arnesen H, Pedersen JI. Serum non-esterified very long-chain PUFA are associated with markers of endothelial dysfunction. *Atherosclerosis* 2002;164:275–281. [PubMed: 12204798]
18. Freedman SD, Blanco PG, Zaman MM, Shea JC, Ollero M, Hopper IK, Weed DA, Gelrud A, Regan MM, Laposata M, Alvarez JG, O'Sullivan BP. Association of cystic fibrosis with abnormalities in fatty acid metabolism. *N. Engl. J Med* 2004;350:560–569. [PubMed: 14762183]
19. Spector AA. Fatty acid binding to plasma albumin. *J. Lipid Res* 1975;16:165–179. [PubMed: 236351]
20. Richieri GV, Kleinfeld AM. Unbound free fatty acid levels in human serum. *J. Lipid Res* 1995;36:229–240. [PubMed: 7751810]
21. Richieri GV, Ogata RT, Kleinfeld AM. A fluorescently labeled intestinal fatty acid binding protein; Interactions with fatty acids and its use in monitoring free fatty acids. *J. Biol. Chem* 1992;267:23495–23501. [PubMed: 1429693]
22. Richieri GV, Ogata RT, Kleinfeld AM. Kinetics of fatty acid interactions with fatty acid binding proteins from adipocyte, heart, and intestine. *J. Biol. Chem* 1996;271:11291–11300. [PubMed: 8626681]
23. Ho SN, Hunt HD, Horton RM, Pullen JK, Pease LR. Site-directed mutagenesis by overlap extension using the polymerase chain reaction. *Gene* 1989;77:51–59. [PubMed: 2744487]
24. Bradford MM. A rapid and sensitive method for the quantitation of microgram quantities of protein utilizing the principle of protein-dye binding. *Anal. Biochem* 1976;72:248–254. [PubMed: 942051]

25. Kampf, JP.; Cupp, D.; Kleinfeld, AM. Different mechanisms of free fatty acid flipflop and dissociation revealed by temperature and molecular species dependence of transport across lipid vesicles. *J. Biol. Chem.* 2006. in press
26. Yuvienco JMS, Dizon EC, Kleinfeld AM, Anwar M, Hiatt M, Hegyi T. Umbilical cord unbound free fatty acid concentration and low Apgar score. *Am. J. Perinatology* 2005;22:429–436.
27. Richieri GV, Ogata RT, Kleinfeld AM. The measurement of free fatty acid concentration with the fluorescent probe ADIFAB: A practical guide for the use of the ADIFAB probe. *Mol. Cell Biochem* 1999;192:87–94. [PubMed: 10331662]
28. Richieri GV, Low PJ, Ogata RT, Kleinfeld AM. Mutants of rat intestinal fatty acid binding protein illustrate the critical role played by enthalpy-entropy compensation in ligand binding. *J. Biol. Chem* 1997;272:16737–16740. [PubMed: 9201976]
29. Richieri GV, Low PJ, Ogata RT, Kleinfeld AM. Thermodynamics of fatty acid binding to engineered mutants of the adipocyte and intestinal fatty acid binding proteins. *J. Biol. Chem* 1998;273:7397–7405. [PubMed: 9516437]
30. Spector AA, Fletcher JE, Ashbrook JD. Analysis of long-chain free fatty acid binding to bovine serum albumin by determination of stepwise binding constants. *Biochemistry* 1971;10:3229–3232. [PubMed: 5165844]
31. Bojesen IN, Bojesen E. exchange efflux of [3H]palmitate from human red cell ghost to bovine serum albumin in buffer. effects of medium volume and concentration of bovine serum albumin. *Biochimica et Biophysica Acta* 1992;2736:185–196. [PubMed: 1420254]
32. Rose H, Conventz M, Fischer Y, Jungling E, Hennecke T, Kammermeier H. Long-chain fatty acid-binding to albumin: re-evaluation with directly measured concentrations. *Biochim. Biophys Acta* 1994;1215:321–326. [PubMed: 7811718]
33. Bojesen IN, Bojesen E. Binding of arachidonate and oleate to bovine serum albumin. *J. Lipid Res* 1994;35:770–778. [PubMed: 8071600]
34. Bojesen IN, Bojesen E. Albumin binding of long chain fatty acids: Thermodynamics and kinetics. *J. Phys. Chem* 1996;100:17981–17985.
35. Elmadhoun BM, Wang GQ, Templeton JF, Burczynski FJ. Binding of [3H]palmitate to BSA. *Am. J. Physiol* 1998;275:G638–G644. [PubMed: 9756491]
36. Demant EJF, Richieri GV, Kleinfeld AM. Stopped-flow kinetic analysis of long-chain fatty acid dissociation from bovine serum albumin. *Biochem. J* 2002;363:809–815. [PubMed: 11964183]
37. Petitpas I, Grune T, Bhattacharya AA, Curry S. Crystal structures of human serum albumin complexed with monounsaturated and polyunsaturated fatty acids. *J. Mol. Biol* 2001;314:955–960. [PubMed: 11743713]
38. Parks JS, Cistola DP, Small DM, Hamilton JA. Interactions of the carboxyl group of oleic acid with bovine serum albumin: a ¹³C NMR study. *J. Biol. Chem* 1983;258:9262–9269. [PubMed: 6874688]
39. Cistola DP, Small DM, Hamilton JA. Carbon 13 NMR studies of saturated fatty acids bound to bovine serum albumin: The filling of individual fatty acid binding sites. *J. Biol. Chem* 1987;262:10971–10979. [PubMed: 3611099]
40. Hamilton JA, Cistola DP. Transfer of oleic acid between albumin and phospholipid vesicles. *Proc. Natl. Acad. Sci USA* 1986;83:82–86. [PubMed: 3455761]
41. Richieri GV, Ogata RT, Kleinfeld AM. Thermodynamics of fatty acid binding to fatty acid-binding proteins and fatty acid partition between water and membranes measured using the fluorescent probe ADIFAB. *J. Biol. Chem* 1995;270:15076–15084. [PubMed: 7797491]
42. Munson PJ, Rodbard D. Number of receptor sites from Scatchard and Klotz graphs: a constructive critique. *Science* 1983;220:979–981. [PubMed: 6302842]

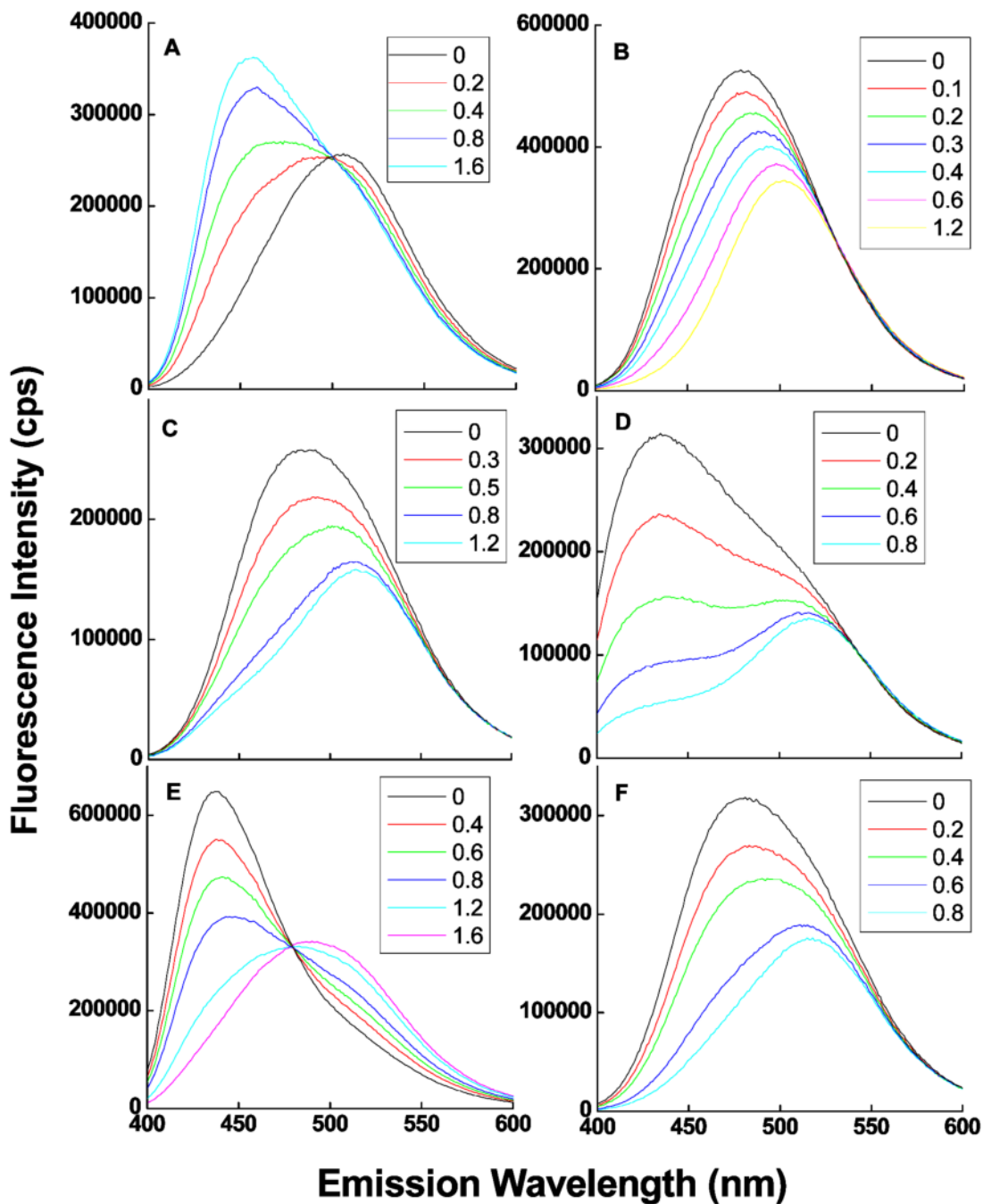


Figure 1. Fluorescence spectra of FFA-specific probes

The set of spectra for each probe represent titrations with increasing concentrations (in μM inserts) of the FFA to which they best respond. (A):L1P8H2 with OA, (B): L2P22G6 with PA (C): L10P7A4 with AA (D):L11P7B3 with SA (E):L13P7B4 with OA and (F):L18P5G12 with LA. For all spectra the excitation wavelength was 375 nm and the probe concentration was 1 μM .

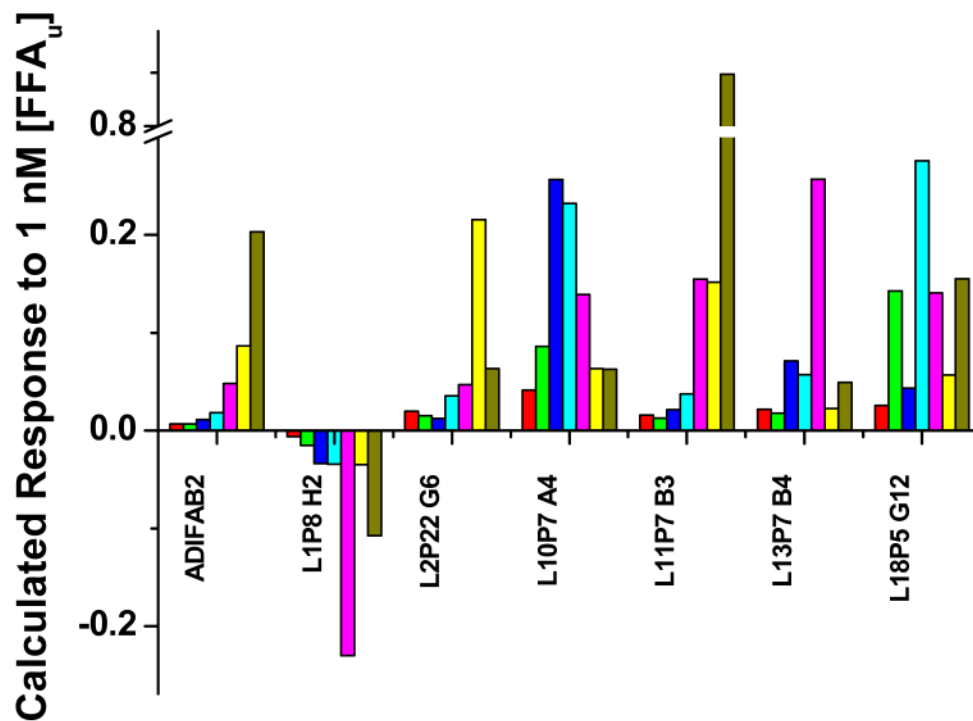


Figure 2. The probe response profiles

Profiles for each probe are represented as the fractional change in R for 1 nM [FFA_u] calculated using the calibration constants in Table 2. For each profile the responses correspond from left to right for the most (POA) to least (SA) soluble FFA. POA – red, LNA – green, AA – blue, LA – cyan, OA – pink, PA – yellow, and SA – brown.

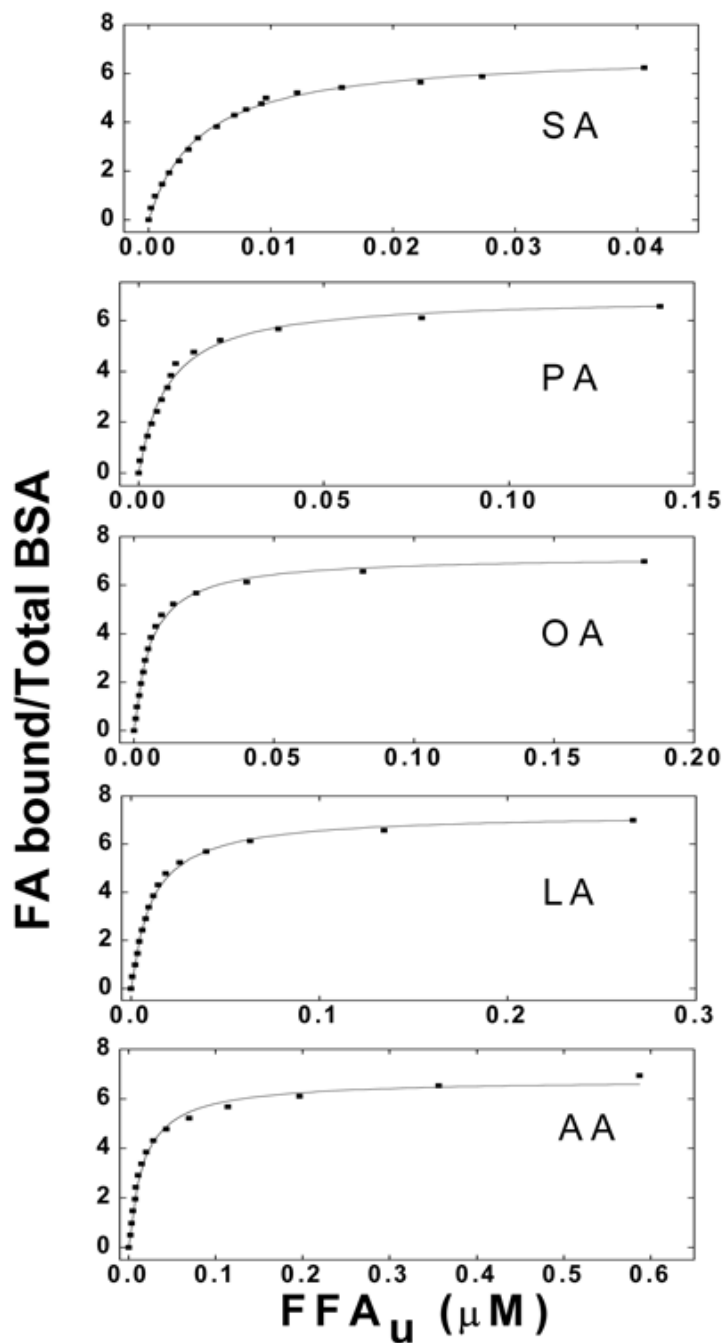


Figure 3. BSA binding isotherms for 5 different FFA

Measured FA bound/total BSA values are shown as solid square symbols and the line through these data represent best fits of the single-class albumin binding model. These results are representative of at least two separate titrations for each FFA.

Table 1

FFA screening profiles for probes.^a

ID	AA	LNA	LA	OA	PA	POA	SA	Mutations
L1P8 H2	-4.17	-4.78	-3.93	-5.38	-1.24	-2.73	-2.29	Y14M L38M L72W
L2P22 G6	3.70	6.73	5.15	3.27	5.88	8.13	1.12	M18I G31Y L72A A73G
L10P7 A4	10.9	10.5	8.90	5.27	2.73	7.51	1.17	Y14L M18L G31Y L72A A73L Y117A
L11P7 B3	8.50	7.99	7.73	9.23	5.33	7.10	6.50	M21F L72A L78V L102V
L13P7 B4	4.42	3.36	3.24	3.62	0.87	2.98	0.50	L72A R106W Q115C
L18P5 G12	11.5	15.8	14.0	8.91	2.76	9.98	2.49	Y14R M18L A73F Y117D

^aResponse profiles (pI) for each of the 6 probes (ID) which were generated by between 3 and 6 amino acid (using single letter notation) substitutions in the wild type rat intestinal FABP.

Table 2

Probe fluorescence calibration constants.^a

	L1P8 H2 0.62	L2P22 G6 0.20	L10P7 A4 0.69	L11P7 B3 0.29	L13P7 B4 0.09	L18P5 G12 0.49
R₀	AA 104	90.6	5.1	248	35.9	47.5
	LNA 217	89.0	13.9	249	149	13.1
	LA 97.5	42.2	4.7	57.6	46.4	9.7
K_d	OA 14.4	33.9	4.9	20.1	10.5	20.0
	PA 45.4	5.6	12.6	13.5	46.7	36.9
	POA 209	87.9	22.3	176	90.3	90.7
	SA 19.2	17.6	9.3	3.2	45.2	11.0
Q	AA 0.24	2.80	1.89	4.70	2.19	4.39
	LNA 0.27	3.75	2.31	5.61	1.83	5.26
	LA 0.25	2.60	2.33	9.00	1.90	4.52
	OA 0.20	2.37	1.60	6.70	2.17	3.57
	PA 0.44	4.00	1.57	6.33	1.68	3.26
	POA 0.47	2.73	1.87	5.10	1.78	4.15
	SA 0.34	2.95	1.57	6.58	1.81	4.12
R_m	AA 0.08	0.83	2.56	7.56	0.57	4.90
	LNA 0.06	1.21	2.65	5.52	0.50	5.36
	LA 0.08	0.99	2.59	5.94	0.52	6.50
	OA 0.07	0.97	1.54	6.39	0.60	5.46
	PA 0.17	1.21	1.60	4.10	0.24	3.82
	POA 0.26	1.15	1.91	4.49	0.39	5.23
	SA 0.12	0.87	1.36	6.02	0.43	3.98

^aThis table lists the binding (K_d) and spectroscopic (Q and R_m) parameters of equation (3) that determine the response of each of the probes to the different FFA.

Table 3Single class BSA-FFA binding parameters.^a

Fatty Acid	K_{d1}^a (nM)	M
AA	16 ± 1	7.2 ± 0.6
LNA	35 ± 1	7.2 ± 0.5
LA	13 ± 2	7.3 ± 0.1
OA	5.9 ± 0.1	7.4 ± 0.3
PA	8.0 ± 0.2	6.9 ± 0.1
POA	38 ± 2	6.6 ± 0.5
SA	4.1 ± 0.2	5.8 ± 0.3

^aThe binding parameters, binding constant (K_{d1}^a) and number of binding sites (M), determined by fitting equation (A5) to the BSA binding isotherms for single fatty acids.

Table 4
 FFA_u distributions determined in mixtures of 4 fatty acids with BSA.^a

	1:1:1:1			30:35:20:15			
	Experiment	Model		Experiment	Model		
	FFA _u (nM)	X (%)	FFA _u (nM)	FFA _u (nM)	X (%)	FFA _u (nM)	X (%)
AA	0.90	29	0.92	1.08	34	1.11	35
OA	0.81	26	0.72	1.21	39	1.01	32
PA	0.81	26	0.79	0.55	17	0.63	20
SA	0.58	19	0.67	0.31	10	0.40	13
Total	3.10		3.10	3.15		3.15	
AA	7.75	39	7.70	9.45	46	9.10	45
OA	3.48	17	3.94	4.60	23	5.40	27
PA	5.32	27	4.97	4.54	22	3.90	19
SA	3.41	17	3.35	1.79	9	1.97	10
Total	20.0		20.0	20.4		20.4	

^a Experimental FFA_u values were determined from two different mixtures (1:1:1:1 and 30:35:20:15) of AA, OA, PA and SA by analyzing the measured probe responses with equation (4). The mixture ratios shown in the first line of the table indicate the relative volume ratios of the FFA:BSA complexes used to prepare the mixtures (Methods) and these are roughly the final FFA_u ratios observed in the mixtures. Two concentrations of total FFA_u (3.1 and 20 nM) were used for each distribution. Model values of FFA_u were calculated using the single class model (Equations (A4 & A6)). Also shown is the fraction of each FFA_u in the mixture (X in %).

Table 5

FFAu distributions determined in mixtures of 5 fatty acids with BSA.^a

	1:1:1:1:1			20:25:30:15:10			25:20:33:19:3			
	Experiment FFA _{ij} (nM)	X (%)	Model FFA _{ij} (nM)	Experiment FFA _{ij} (nM)	X (%)	Model FFA _{ij} (nM)	Experiment FFA _{ij} (nM)	X (%)	Model FFA _{ij} (nM)	
AA	0.200	22	0.191	21	0.170	19	0.191	21	0.249	26
LA	0.183	20	0.189	21	0.235	26	0.236	26	0.196	21
OA	0.106	12	0.175	19	0.230	25	0.262	29	0.299	32
PA	0.253	28	0.182	20	0.190	21	0.136	15	0.207	22
SA	0.164	18	0.170	19	0.085	9	0.085	9	0.028	3
Total	0.907		0.907		0.910		0.910		0.949	
AA	0.727	23	0.737	23	0.776	24	0.748	23		
LA	0.659	21	0.707	22	0.820	25	0.896	27		
OA	0.622	20	0.573	18	0.930	28	0.868	27		
PA	0.706	22	0.633	20	0.535	16	0.480	15		
SA	0.464	15	0.531	17	0.203	6	0.268	8		
Total	3.18		3.18		3.26		3.26			
AA	6.22	32	5.63	29	5.52	29	5.39	28		
LA	4.71	24	4.94	25	6.25	32	5.91	31		
OA	2.51	13	2.89	15	3.76	20	4.16	22		
PA	3.20	16	3.64	19	2.35	12	2.62	14		
SA	2.93	15	2.46	13	1.37	7	1.18	6		
Total	19.6		19.6		19.3		19.3			

^a Experimental FFA_{ij} values were determined from three different mixtures (1:1:1:1:1, 20:25:30:15:10 and 25:20:33:19:3) of AA, LA, OA, PA and SA by analyzing the measured probe responses with equation (4). The mixture ratios shown in the first line of the table indicate the relative volume ratios of the FFA:BSA complexes used to prepare the mixtures (Methods) and these are roughly the final FFA_{ij} ratios observed in the mixtures. Except for the 25:20:33:19:3 (0.9 nM), three concentrations of total FFA_{ij} (0.9, 3.2 and 20 nM) were used for each distribution. Model values of FFA_{ij} were calculated using the single class model (Equations (A4 & A6)). Also shown is the fraction of each FFA_{ij} in the mixture (X in %).

Table 6Estimated experimental errors in FFA_{ui} in percent.^a

FFA	20nM	3nM	0.9nM
AA	7	8	10
LA	<1	3	4
OA	6	16	30
PA	3	4	10
SA	1	3	1

^aError estimates for the FFA_{ui} were determined using a 1% error in R (see Methods) and the results are shown for the mixtures of five fatty acids at three different concentrations of Table 5.

Table 7
 FFA_u and total FFA distributions of two mixtures of 5 fatty acids with BSA.^a

	1:1:1:1:1						20:25:30:15:10					
	Experiment			Model			Experiment			Model		
	FFA _u (mM)	X %	Total FFA (μ M)	FFA _u (mM)	X %	Total FFA (μ M)	FFA _u (mM)	X %	Total FFA (μ M)	FFA _u (mM)	X %	Total FFA (μ M)
AA	0.73	23	115	0.74	10	122	0.78	24	115	0.75	23	124
LA	0.66	21	169	0.71	15	171	0.82	25	212	0.90	27	217
OA	0.62	20	267	0.57	24	262	0.93	28	400	0.87	27	406
PA	0.71	22	240	0.63	21	219	0.54	16	180	0.48	15	167
SA	0.46	15	330	0.53	29	331	0.20	6	165	0.27	8	168
Total	3.2		1121	3.2		1108	3.3		1072	3.3		1082

^a Experimental values of the total FFA profiles were determined from the amount of FFA that was used to make each FFA:BSA complex. The mixture ratios shown in the first line of the table indicate the relative volume ratios of the FFA:BSA complexes used to prepare the mixtures (Methods) and these are roughly the FFA_u ratios observed in the mixtures. (Note that the total FFA concentrations in Table 7 are the concentrations before the mixtures were diluted 100 fold in Measurement Buffer.) Model values of the total FFA profiles were calculated from the single class BSA binding model (Equation A6).